Computational and experimental investigations into the conformations of cyclic tetra-α/β-peptides

Oakley, Mark T.; Oheix, Emmanuel; Peacock, Anna F. A.; Johnston, Roy L.

DOI:
10.1021/jp4043039

THE JOURNAL OF PHYSICAL CHEMISTRY B

Article

pubs.acs.org/JPCB

Computational and Experimental Investigations into the Conformations of Cyclic Tetra-α/β-peptides

Mark T. Oakley,* Emmanuel Oheix, Anna F. A. Peacock,* and Roy L. Johnston*

School of Chemistry, University of Birmingham, Edgbaston, Birmingham, B15 2TT, U.K.

Supporting Information

ABSTRACT: We present a combined computational and experimental study of the energy landscapes of cyclic tetra-α/β-peptides. We have performed discrete path sampling calculations on a series of cyclic tetra-α/β-peptides to obtain the relative free energies and barriers to interconversion of their conformers. The most stable conformers of cyclo-[(β-Ala-Gly)$_2$] contain all-trans peptide groups. The relative energies of the cis isomers and the cis−trans barriers are lower than in acyclic peptides but not as low as in the highly strained cyclic α-peptides. For cyclic tetra-α/β-peptides containing a single proline residue, of the type cyclo-[β-Ala-Xaa-β-Ala-Pro], the energy landscapes show that the most stable isomers containing cis and trans β-Ala-Pro have similar free energies and are separated by barriers of approximately 15 kcal mol^{-1}. We show that the underlying energy landscapes of cyclo-[β-Ala-Lys-β-Ala-Pro] and cyclo-[β-Ala-Ala-β-Ala-Pro] are similar, allowing the substitution of the flexible side chain of Lys with Ala to reduce the computational demand of our calculations. However, the steric bulk of the Val side chain in cyclo-[β-Ala-Val-β-Ala-Pro] affects the conformations of the ring, leading to significant differences between its energy landscape and that of cyclo-[β-Ala-Ala-β-Ala-Pro]. We have synthesized the cyclic peptide cyclo-[β-Ala-Lys-β-Ala-Pro], and NMR spectroscopy shows the presence of conformers that interconvert slowly on the NMR time scale at temperatures up to 80 °C. Calculated circular dichroism (CD) spectra for the proposed major isomer of cyclo-[β-Ala-Ala-β-Ala-Pro] are in good agreement with the experimental spectra of cyclo-[β-Ala-Lys-β-Ala-Pro], suggesting that the Ala cyclic tetrapeptide is a viable model for the Lys analogue.

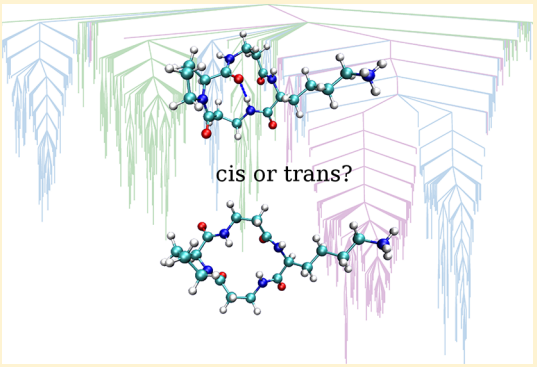

INTRODUCTION

All but the simplest of molecules exist as a mixture of conformers. This is particularly important for biomolecules such as polypeptides. Here we investigate head-to-tail cyclic peptides, which are a class of molecules that are of interest from a pharmaceutical perspective for their biological properties, such as immunosuppression[1] and activity against microbes,[2,3] tumors,[4] and amyloid fibrils.[5] Cyclic tetrapeptides, of which there are many biologically active examples,[3,4,6] have particularly interesting conformational dynamics, with several conformers interconverting slowly.[7,6] A range of computational methods have been used to explore the conformations of cyclic peptides.[8−12] Most of these have focused on locating stable conformers for these compounds, but to fully understand their conformational chemistry we must also study the transition states governing the interconversion of conformers. Discrete path sampling is a method for generating the low-lying minima and the transition states connecting them.[13−15] We have previously used this method to explore the energy landscape of some small cyclic α-peptides.[12]

The conformational behavior of cyclic peptides is particularly interesting with respect to cis−trans isomerization.[9,12,16] In acyclic peptides, the peptide bonds tend to favor trans conformations, with only 0.03% of the nonproline residues adopting cis conformations.[17] However, proline (Pro) residues commonly lead to the formation of isomeric mixtures, with about 5% of Xaa-Pro peptide bonds in proteins present in the cis conformation.[17] The tendency to form the cis conformation is highly dependent on the amino acid sequence. For example, the presence of an electron-rich aromatic side chain on the adjacent residue promotes the formation of the cis conformer.[18] Cis−trans isomerization of Xaa-Pro can prevent or reduce the rate of protein folding; therefore, the presence of both cis and trans Pro isomers for a given peptide residue is often a characteristic of unfolded proteins.[19] Upon folding of the protein domain, only one (either cis or trans) of the two isomers of that particular peptide bond is present. In some signaling proteins, cis−trans isomerization of a single Xaa-Pro peptide bond controls the interconversion of two states of the protein.[20,21] In the absence of external stimuli, the high energetic barrier to interconversion of the cis and trans peptides (~20 kcal mol^{-1} for most amino acids or ~15 kcal mol^{-1} for Xaa-Pro) is largely independent of solvent polarity[22] or temperature.[23,24] Some enzymes (e.g. cyclophillins) are able

Received: May 1, 2013
Revised: June 10, 2013
Published: June 12, 2013

dx.doi.org/10.1021/jp4043039 | J. Phys. Chem. B 2013, 117, 8122−8134

to promote protein folding by lowering the cis−trans isomerization activation barrier.[25]

Cyclization has a significant effect on the cis−trans isomerization of small cyclic peptides, with a decrease in the size of the ring leading to an increase in the occupation of the cis peptide conformers.[9] Our discrete path sampling calculations show that smaller ring sizes lead to a lower barrier to cis−trans isomerization.[12] The strain in the 12-membered rings of cyclic tetra-α-peptides causes them to have very different energy landscapes to either acyclic or larger cyclic peptides, with the cis and trans isomers very close in energy. The barriers to cis−trans isomerization are also substantially lower due to distortion of the peptide bond, while the barriers to rotation of the other torsion angles in the macrocycle are larger due to steric crowding.

Ring strain makes closure of the 12-membered ring of a cyclic tetra-α-peptide rather difficult, and novel strategies, such as ring contraction or metal templating, need to be employed in their synthesis.[26−34] β-Peptide residues, such as β-alanine (β-Ala), have an extra methylene group in their peptide backbones. Including two of them in a cyclic tetrapeptide gives a larger 14-membered ring, which is less strained and therefore more accessible synthetically. These non-native cyclic tetra-α/β-peptides have a ring structure similar to the widely used cyclam ligand and can be used as novel ligands for metal complexation.[35] Including a proline residue, which is able to adopt a cis conformation and bring the two termini of the peptide close together, further increases the ease of cyclization.[33] Cyclic tetra-α/β-peptides that have been synthesized previously include cyclo-[(β-Ala-Ala)$_2$],[36] cyclo-[β-Ala-Ala-β-Ala-Pro],[36] cyclo-[(β-Ala-Pro)$_2$],[36−38] and cyclo-[β-Ala-Val-β-Ala-Pro].[39]

Here, we investigate whether the unusual conformational features of cyclic tetra-α-peptide energy landscapes are retained in cyclic tetrapeptides containing two β-amino acid residues. We report the synthesis of the cyclic tetrapeptide cyclo-[β-Ala-Lys-β-Ala-Pro] using solid-phase methods, with the growing peptide chain anchored to the resin via the side chain of the lysine (Lys) residue. Cyclization of the peptide is performed on-resin under pseudo-high-dilution conditions[40−42] to minimize the likelihood of intermolecular reactions leading to cyclic octapeptides or larger polypeptides. Nuclear magnetic resonance (NMR) and circular dichroism (CD) spectroscopies were used to study the conformations adopted by this cyclic peptide.

We use discrete path sampling to investigate the free energy landscapes of a series of cyclic tetra-α/β-peptides, starting with cyclo-[(β-Ala-Gly)$_2$] and building up toward cyclo-[β-Ala-Lys-β-Ala-Pro]. We compare these to cyclic tetra-α-peptides and acyclic peptides to understand the effect of β-amino acid residues on the underlying energy landscapes. Replacing the flexible Lys side chain in cyclo-[β-Ala-Lys-β-Ala-Pro] with less flexible side groups substantially reduces the number of stationary points to be explored. We present the energy landscapes of cyclo-[β-Ala-Ala-β-Ala-Pro] and cyclo-[β-Ala-Val-β-Ala-Pro], which both have side chains that are less flexible than Lys. The Val residue has a sterically demanding isopropyl side chain in close proximity to the cyclic peptide backbone, which may affect the conformations of the ring. We also present calculated CD spectra[43−45] derived from the energy landscapes of cyclo-[β-Ala-Ala-β-Ala-Pro] and show that they are in good agreement with the experimental CD spectra of cyclo-[β-Ala-Lys-β-Ala-Pro].

COMPUTATIONAL METHODS

Free Energy Landscapes. The energies of all structures were evaluated using the AMBER ff03 force field.[46−48] Solvent effects were modeled using the generalized Born implicit solvation method.[49] We have previously shown that the energies of cyclic tetrapeptide conformers calculated with the AMBER ff03 force field are in good agreement with those calcualted with density functional theory at the B3LYP/6-31G* level.[12] Parameters for the unnatural amino acid β-Ala were needed for these calculations. The α- and β-carbon atoms were both assigned as atom type CT, and the hydrogen atoms attached to these were assigned as type H1. Mulliken charge analysis[50] at the HF/6-31G* level was performed on both Ala and β-Ala using NWChem.[51] The force field charges for β-Ala were obtained by adjusting the Ala charges based on the difference between the two sets of Mulliken charges. These parameters are available as Supporting Information. All structures are visualized using the VMD molecular graphics program.[52]

The energy landscapes of the cyclic peptides were explored with discrete path sampling[13−15] as implemented in the PATHSAMPLE software.[53] For each cyclic peptide, an initial database of minima was generated using the basin-hopping algorithm[54] in GMIN.[55] Pairs of minima were then connected via doubly nudged elastic band calculations[56] in OPTIM[57] to locate a pathway between them. This pathway may consist of a single transition state or a sequence of several minima and transition states. Candidate transition states were then optimized by hybrid eigenvector following[58−60] in OPTIM.[57] These are then added to a database of stationary points, and a connection attempt is made on another pair of minima. Pairs of minima for connection were chosen using the missing connections algorithm.[61] Later, pairs of minima were connected using the UNTRAP method to remove any artificial frustration.[62] The search continued until no new low-lying minima or transition states were found for several connection attempts.

The energy landscapes are visualized as disconnectivity graphs,[63,64] in which the minima are partitioned into disjoint sets using the energies of the connecting transition states. A node on a disconnectivity graph represents the energy of the highest transition state on the lowest pathway connecting a pair of minima. This allows easy visualization of a large network of minima and transition states. All of the disconnectivity graphs presented here show free energy landscapes calculated at 298 K.[65,66] To obtain the free energy, we use the harmonic approximation to include the effect of vibrational entropy. The free energy of a minimum, F_i, or transition state, $F^\dagger$, at temperature T is given by

$$F_i(T) = E_i + k_B T \ln(h\bar{\nu}_i/n_i^* k_B T)^\kappa \quad (1)$$

$$F^\dagger(T) = E^\dagger + k_B T \ln(h\bar{\nu}^\dagger/n^{*\dagger} k_B T)^{\kappa-1} \quad (2)$$

where $\bar{\nu}$ is the geometric mean normal-mode frequency and κ is the number of vibrational degrees of freedom. Some of the peptides presented here, such as cyclo-[(β-Ala-Gly)$_2$], are highly symmetrical, with groups of symmetry equivalent stationary points. During the discrete path sampling calculations, the permutation-inversion isomers of each stationary point are combined, and permutational entropy is taken into account in the free energy calculations, with n^* being the number of permutation-inversion isomers.[67,68]

dx.doi.org/10.1021/jp4043039 | J. Phys. Chem. B 2013, 117, 8122−8134

We present calculations on the cyclic-α/β-peptides cyclo-[(β-Ala-Gly)$_2$], cyclo-[β-Ala-Ala-β-Ala-Pro], cyclo-[β-Ala-Val-β-Ala-Pro], and cyclo-[β-Ala-Lys-β-Ala-Pro]. If we assume that each rotatable bond in the side chain can occupy one of three conformations, cyclo-[β-Ala-Val-β-Ala-Pro] should have three times as many minima as cyclo-[β-Ala-Ala-β-Ala-Pro], and cyclo-[β-Ala-Lys-β-Ala-Pro] should have $3^4 = 81$ times as many minima as cyclo-[β-Ala-Ala-β-Ala-Pro]. The number of minima makes discrete path sampling calculations for cyclo-[β-Ala-Lys-β-Ala-Pro] difficult, and we present a partial energy landscape for this cyclic peptide. For comparison, the free energy landscapes of some of the cyclic- and acyclic-α-peptides in our previous study were also generated using the published databases of stationary points.[12] The PATHSAMPLE databases of stationary points for cyclo-[(β-Ala-Gly)$_2$], cyclo-[β-Ala-Ala-β-Ala-Pro], cyclo-[β-Ala-Val-β-Ala-Pro], and cyclo-[β-Ala-Lys-β-Ala-Pro] are available at http://www.stchem.bham.ac.uk/~moakley/.

Circular Dichroism (CD) Calculations. The CD spectra of the cyclic peptides were calculated using the matrix method,[43−45,69−71] which treats a polypeptide as a collection of amide chromophores that interact electrostatically. The transition properties of the peptide groups were parametrized through CASSCF/CASPT2 calculations on *N*-methylacetamide.[72] In the wavelength range 200−250 nm, the CD spectra of peptides are dominated by the amide $n \rightarrow \pi^*$ and $\pi \rightarrow \pi^*$ transitions. Here, we use the simplest peptide parameters including only these transitions. Additional parameters for higher-energy local transitions[43] or charge-transfer transitions[73] are unnecessary as these occur at shorter wavelengths than the recorded experimental spectra.

By assuming that the chromophores only interact electrostatically, the matrix method does not include any through-bond interactions. Also, any changes to the transition properties of the amide groups due to changes in the solvent[74] or geometrical distortion are not taken into account. Despite these limitations, the matrix method works well for molecules of a similar size to the ones in this paper. For example, the transition energies and dipole moments of glycouril, a cyclic diurea, from matrix method calculations, ab initio calculations, and experimental measurements are in good agreement.[75] In principle, the CD spectra can be calculated using time-dependent density functional theory (TDDFT). However, widely used functionals, such as B3LYP, represent charge-transfer transitions poorly.[76] This is a significant problem for peptides because charge-transfer transitions, which should occur at relatively high energies, are calculated to be close to the local $\pi \rightarrow \pi^*$ transitions.

A major advantage of matrix method calculations is that they require little computational effort. Therefore, the CD spectra of all minima for the compounds presented here can be generated rapidly. The CD spectrum corresponding to a funnel on the energy landscape is taken as the sum of the calculated CD spectra for all minima within that funnel weighted by the probability, P_s, of being in the catchment basin of a minimum s:

$$P_s = \frac{e^{-\beta F_s}}{\sum_s e^{-\beta F_s}} \tag{3}$$

where F_s is the free energy of that basin and $\beta = 1/k_B T$. The sum is taken over all states found by the discrete path sampling algorithm. Gaussian curves with a half width of 12.5 nm are then added to the resulting line spectra to produce the CD spectra presented here.

EXPERIMENTAL METHODS

General Experimental. Fmoc-protected α-amino acids, peptide grade solvents (DMF, DCM, NMP, 20% piperidine in DMF), *N*,*N*-diisopropylethylamine (DIEA), 2-chlorotrityl resin, and HBTU were obtained from AGTC Bioproducts. Fmoc-β-Ala was obtained from Novabiochem. HPLC grade solvents (DCM, acetonitrile, water, acetic acid, methanol) were purchased from Fisher Scientific and allyl bromide, $Pd(PPh_3)_4$, $PhSiH_3$, and TFA from ACROS Organics. Sodium diethyldithiocarbamate was purchased from Sigma-Aldrich. All chemicals were used directly as received, apart from DCM which was refluxed over CaH_2 prior to use. ESI-TOF MS were recorded on a Microwaters LCT TOF spectrometer equipped with a 3000 V capillary voltage and a cone voltage of 35 V. MALDI-TOF MS were recorded on a Bruker Biflex IV equipped with a nitrogen laser (337 nm). ESI samples were prepared in a water/methanol/acetic acid mixture (50:50:0.1), and MALDI was performed with 2,5-dihydroxybenzoic acid as the matrix. The MALDI-TOF instrument was calibrated over the range 1000−1600 with a protein mixture containing Angiotensin II (m/z = 1046.54180), Angiotensin I (m/z = 1296.68748), substance P (m/z = 1347.73543), and Bombesin (m/z = 1619.82235) using a quaternary fit. All spectra were recorded in positive mode. Elemental analyses were recorded on an EA CHNS 1110; combustion was performed at 950 °C; and the data were treated using Eager 300 software. ^{1}H and ^{13}C NMR spectra for characterization were collected on a Bruker AVANCEIII 300 (300 MHz ^{1}H), AVANCEIII 400 (400 MHz ^{1}H and 100 MHz ^{13}C), or DRX500 (500 MHz ^{1}H and 125 MHz ^{13}C) spectrometer equipped with a 5 mm probe. TOCSY, NOESY, and HSQC spectra of cyclo-[β-Ala-Lys-β-Ala-Pro] were recorded in H_2O:D_2O (90:10) at 300 K on the Bruker DRX500. The variable-temperature NMR experiments were recorded in MeOD-d_4 or DMSO-d_6 on the Bruker AVANCE DRX400 (400 MHz ^{1}H). Spectra were referenced based on previous measurements involving an external trimethylsilyl propionate (TSP) reference dissolved in D_2O or the solvent peak for MeOD-d_4 or DMSO-d_6 solutions. Chemical shifts (δ) are given in parts per million (ppm) downfield of the methyl peak of the trimethylsilyl group at 0 ppm. Data were processed using Bruker Topspin version 2.1 (300 and 400 MHz), Topspin version 1.3 (500 MHz), or Mestrenova Lite version 5.2.5. Circular dichroism (CD) spectra were recorded in 1 mm path length quartz cuvettes on a Jasco J-715 spectropolarimeter. The observed ellipticity in millidegrees was converted into molar ellipticity (θ) and is reported in units of deg cm^2 dmol^{-1} res^{-1}. Stock solutions were freshly prepared in methanol (16 mM) and water (2.5 mM) and aliquots used for preparation of CD samples. The concentration of aqueous stock solution was based on mass, and the concentration of the methanolic stock solution was determined from the ellipticity at 220 nm for cyclo-[β-Ala-Lys-β-Ala-Pro] in 50/50 water:methanol mixtures. To prevent solvent evaporation, methanol stock solutions were stored at −18 °C between uses.

Allyl 2-[(9-Fluorenylmethoxy)carbonylamino]-6-[*tert*-butoxycarbonylamino] Hexanoate (Fmoc-Lys(Boc)-OAll). Two equiv. of DIEA (0.74 mL, 4.25 mmol) was added to a mixture of Fmoc-Lys(Boc)-OH (1.00 g, 2.14 mmol) and allyl bromide (5 mL, 57.8 mmol), and the suspension was refluxed for 3 h. Ethyl acetate (100 mL) was added to dissolve

dx.doi.org/10.1021/jp4043039 | J. Phys. Chem. B 2013, 117, 8122−8134

the mixture, which was subsequently washed with a saturated sodium hydrogen carbonate aqueous solution (3 × 50 mL) and brine (3 × 50 mL). The organic phase was dried ($MgSO_4$) and the drying agent removed by filtration before removing the solvent under reduced pressure to produce a pale yellow solid. This was triturated with cold diethyl ether, recovered by filtration, and air-dried to yield a white powder (1.00 g, 92%). ^{1}H NMR (300 MHz, $CDCl_3$, 20 °C, relative to TMS): 7.76 (d, ^3J = 7.5 Hz, 2 H, H_{Ar} Fmoc), 7.60 (d, ^3J = 7.3 Hz, 2 H, H_{Ar} Fmoc), 7.39 (t, ^3J = 7.5 Hz, 2 H, H_{Ar} Fmoc), 7.30 (t, ^3J = 7.4 Hz, 2 H, H_{Ar} Fmoc), 5.90 (m, 1 H, H_{CH} allyl), 5.46 (br d, ^3J = 7.8 Hz, 1 H, H_{NH} side chain), 5.33 (dd, ^3J = 1.2 Hz, ^2J = 17.2 Hz, 1 H, H_{CH2} allyl), 5.25 (dd, ^3J = 1.1 Hz, ^2J = 10.4 Hz, 1 H, H_{CH2} allyl), 4.64 (d, ^3J = 5.7 Hz, 2 H, H_{CH2} allyl), 4.61−4.30 (m, 4H, H_{CH2O} Fmoc, H_α Lys, H_{NH} amide), 4.22 (t, ^3J = 7 Hz, 1 H, $H_{fluorenyl}$ Fmoc), 3.10 (t, ^3J = 6 Hz, 2 H, H_ε Lys), 1.95−1.30 (m, 6 H, $H_{\beta,\gamma,\delta}$ Lys), 1.43 (s, 9 H, H_{CH3} Boc). These values are consistent with those previously reported,[77] except that our multiplet (4.61−4.30 ppm) integrates for 4 protons rather than 2 as reported in the literature. MS (MALDI-TOF) m/z 546.81 ($[M+K]^+$, 40%), 530.83 ($[M+Na]^+$, 100%), 474.73 ($[M-C_4H_8+Na]^+$, 5%), 408. 68 ($[M-C_5H_8O_2]^+$, 53%); MS (ES+) m/z 531.32 ($[M+Na]^+$, 100%), 475.28 ($[M-C_4H_8+Na]^+$, 8%).

Allyl 2-[(9-Fluorenylmethoxy)carbonylamino]-6-aminohexanoate (Fmoc-Lys-OAll). TFA (15 mL) was slowly added to a solution of Fmoc-Lys(Boc)-OAll (1.00 g, 1.97 mmol) in DCM (15 mL) and stirred at room temperature for 2.5 h. The reaction mixture was then concentrated under reduced pressure and chased with Et_2O (5 × 10 mL) and finally dried in vacuo, to afford a pale yellow powder (1.03 g, 91%). Determined to be 90% pure by analytical C18-HPLC. ^{1}H NMR (400 MHz, $CDCl_3$, 25 °C, relative to TMS): 7.95 (br. s, 2.7 H_{NH2} side chain), 7.72 (d, ^3J = 7.5 Hz, 2 H, H_{Ar} Fmoc), 7.56 (d, ^3J = 7.3 Hz, 2 H, H_{Ar} Fmoc), 7.36 (t, ^3J = 7.4 Hz, 2 H, H_{Ar} Fmoc), 7.27 (t, ^3J = 7.5 Hz, 2 H, H_{Ar} Fmoc), 5.85 (m, 1 H, H_{CH} allyl), 5.66 (d, ^3J = 8.2 Hz, 1 H, H_{NH} amide), 5.28 (d, ^2J = 17.2 Hz, 1 H, H_{CH2} allyl), 5.21 (d, ^2J = 10.4 Hz, 1 H, H_{CH2} allyl), 4.59 (d, ^3J = 5.5 Hz, 2 H, H_{CH2O} allyl), 4.58−4.36 (m, 1 H, H_α Lys), 4.34 (m, 2 H, H_{CH2O} Fmoc), 4.17 (m, 1 H, H_{Ar} Fmoc), 2.92 (br. s, 2 H, H_ε Lys), 1.87−1.30 (m, 6 H, $H_{\beta,\gamma,\delta}$ Lys). ^{13}C NMR (100 MHz, $CDCl_3$, 25 °C, relative to TMS): 172.16 ($C_{C=O}$ Lys), 156.39 ($C_{C=O}$ Fmoc), 143.85 (C_{Ar} Fmoc), 141.40 (C_{Ar} Fmoc), 131.49 (C_{CH} allyl), 127.87 (C_{Ar} Fmoc), 127.21 (C_{Ar} Fmoc), 125.20 (C_{Ar} Fmoc), 120.11 (C_{Ar} Fmoc), 119.16 (C_{CH} allyl), 67.28 (C_{CH2O} Fmoc), 66.26 (C_{CH2O} allyl), 53.80 (C_α Lys), 47.18 (C_{Ar} Fmoc), 39.62 (C_ε Lys), 31.91 (C_β Lys), 26.94 (C_δ Lys), 22.24 (C_γ Lys). MS (MALDI-TOF) m/z 408.85 ($[M+H]^+$, 31%), 430.85 ($[M+Na]^+$, 100%), 446.79 ($[M+K]^+$, 8%), 813.00 ($[M_2-2H]^+$, 6%). MS (ES+) m/z 409.6 ($[M+H]^+$, 100%), 431.6 ($[M+Na]^+$, 16%). Elemental analysis calcd (%) for $C_{26}H_{29}F_3N_2O_6$ (Fmoc-Lys-OAll + TFA): C, 59.76; H, 5.59; N, 5.36. Found: C, 59.73; H, 5.27; N, 5.35.

Fmoc-Lys(resin)-OAll. Two equiv. of DIEA (239 μL; 1.37 mmol) was added to a solution of Fmoc-Lys-OAll (280 mg, 0.685 mmol) in dry DCM. The solution was stirred for 5 min and 2-chlorotrityl resin (1.431 g; 1.3−1.5 mmol/g; 1.86−2.15 mmol) added. The mixture was stirred at rt for 2 h and the resin removed by filtration and washed with DMF (20 mL), a mixture of DCM−MeOH−DIEA (17:2:1) (2 × 20 mL), DMF (5 × 20 mL), DCM (5 × 20 mL), and finally diethyl ether (20 mL). The lysine-loaded resin was dried in a desiccator overnight and the loading rate subsequently determined by measuring the release of the Fmoc group by UV−visible spectroscopy using a previously reported method.[78]

Fmoc-β-Ala-Pro-β-Ala-Lys(resin)-OAll. The linear tetrapeptide was prepared on resin by iterative coupling and deprotections, separated by washings (5 × 25 mL of DMF, 5 × 25 mL of DCM, and finally 3 × 25 mL of Et_2O), for all Fmoc-L-amino acids, using standard Fmoc-amino acid solid-phase peptide synthesis protocols.[78]

Fmoc-β-Ala-Pro-β-Ala-Lys(resin)-CO_2H. The allyl protecting group (OAll) was removed by adding 24 equiv of $PhSiH_3$ (1.74 mL, 14.2 mmol) to a mixture of Fmoc-β-Ala-Pro-β-Ala-Lys(resin)-OAll (1.97 g) in dry DCM (ca. 15 mL). A solution of $Pd(PPh_3)_4$ (170.4 mg, 0.15 mmol, 0.25 equiv) dissolved in the minimum volume (ca. 7 mL) of dry DCM was added and the suspension stirred at rt under a nitrogen atmosphere for 45 min. The resin was recovered by filtration and washed with dry DCM (25 mL). This process was repeated twice to ensure total deprotection. The resin was finally washed with a solution of 0.5% sodium diethyldithiocarbamate in DMF (2 × 20 mL), DMF (5 × 25 mL), DCM (5 × 25 mL), and diethyl ether (3 × 25 mL).

H_2N-β-Ala-Pro-β-Ala-Lys(resin)-CO_2H. The Fmoc group was removed by stirring the resin in 20% piperidine in DMF (25 mL) for 45 min at rt. This process was repeated twice to ensure complete Fmoc removal. The resin was recovered by filtration and washed with DMF (5 × 25 mL), DCM (5 × 25 mL), and diethyl ether (5 × 25 mL).

Cyclo-[β-Ala-Pro-β-Ala-Lys](resin). On-resin cyclization was performed by the successive addition of DMF (20 mL), 2 equiv of HBTU (448 mg, 1.18 mmol), and 4 equiv of DIEA (411 μL, 2.36 mmol) to the resin, which was stirred under an inert nitrogen atmosphere at 4 °C for 1 h, followed by 2 h at rt. The resin was recovered by filtration and washed with DMF (5 × 25 mL), DCM (10 × 25 mL), and diethyl ether (5 × 25 mL).

Cyclo-[β-Ala-Lys-β-Ala-Pro]. The cyclic peptide was cleaved from the resin by the addition of 20 mL of cleavage mixture TFA:H_2O (95:5) and stirring at rt for 2 h. The resin was removed by filtration and washed with TFA (10 mL) and the filtrate reduced to dryness in vacuo. The solid was redissolved in water (ca. 15 mL) and purified by semi-preparative reversed-phase C18-HPLC eluted with a solvent mixture altered with a linear gradient from 0.05% TFA in water to 0.05% TFA in CH_3CN/H_2O (20:80) over 60 min. HPLC fractions were lyophilized to yield a white solid (34 mg, 14%). MS (MALDI-TOF) m/z 367.91 ($[M+H]^+$, 94%), 389.89 ($[M+Na]^+$, 100%), 405.86 ($[M+K]^+$, 35%). Elemental analysis calcd (%) for $C_{17}H_{29}N_5O_4$: C, 55.57; H, 7.96; N, 19.06. Found: C, 55.99; H, 8.49; N, 19.26.

RESULTS AND DISCUSSION

Energy Landscape of Cyclo-[(β-Ala-Gly)$_2$]. We compare the relative free energies of the most stable isomers of cyclo-[(β-Ala-Gly)$_2$] containing trans and cis peptides and the barriers to their interconversion, with cyclo-[Gly_4] in Table 1. We also compare them to the acyclic peptide Ace-Gly_3-NMe, which contains four amide bonds and therefore can be directly compared to cyclic tetrapeptides. The free energies of cyclo-[Gly_4] and Ace-Gly_3-NMe were calculated from our previously published databases of stationary points.[12] The most stable conformers of cyclo-[(β-Ala-Gly)$_2$] have all of the peptide groups in the trans conformation. The most stable conformers containing a cis peptide lie 3.9 kcal mol^{-1} above the global minimum and are separated from it by barriers of 18.2 kcal

dx.doi.org/10.1021/jp4043039 | J. Phys. Chem. B 2013, 117, 8122−8134

Table 1. Free Energies of the Most Stable Structures Containing Cis Peptides in Cyclic and Acyclic Tetrapeptides Relative to the All-Trans Global Minima[a]

	number of *cis*-amide bonds				
sequence	1	2	3	4	cis−trans barrier
cyclo-[Gly_4][12]	2.5	5.0	10.7	16.4	14.9
cyclo-[(β-Ala-Gly)$_2$]	3.9	10.6	15.2	19.9	18.2
Ace-Gly_3-NMe[12]	4.2	9.3	14.1	18.8	18.7

[a]Also shown are the energies of the lowest trans−cis transition states. All energies are in kcal mol^{-1}.

mol^{-1} (Table 1). The relative energies of the cis and trans isomers in cyclo-[(β-Ala-Gly)$_2$] are closer than in the acyclic peptide, and the barriers to their interconversion are smaller. However, the trans−cis barriers are larger than those in cyclo-[Gly_4]. Strain has some influence on the energy landscapes of cyclic tetra-α/β-peptides but to a much lesser extent than for cyclic tetra-α-peptides.

There are 12 structures that contribute more than 5% to the equilibrium population of cyclo-[(β-Ala-Gly)$_2$] (Figure 1). Many of these are degenerate, and there are only four symmetry-unique conformers: two doubly degenerate C_2-symmetric structures and two quadruply degenerate structures with C_1 symmetry. Some of these structures contain one or two hydrogen bonds as part of a γ-turn. The structure containing two hydrogen bonds (Figure 1d) is close to Vass's proposed global minimum structure for cyclic tetra-α/β-peptides.[36] All of these conformers have similar placements of the β-Ala-Gly peptide bonds, which lie in the plane of the ring with the oxygen atoms pointing outward. The main differences between the conformers are in the orientations of the Gly-β-Ala peptide groups relative to the plane of the ring. The calculated barriers to rotations of these peptide groups are 4−6 kcal mol^{-1} (Figure 1). At equilibrium, conformers containing all-trans peptide groups make up more than 99.9% of the total population.

Energy Landscape of Cyclo-[β-Ala-Ala-β-Ala-Pro]. In water, the free energy landscape of cyclo-[β-Ala-Ala-β-Ala-Pro] has two low-lying funnels separated by a barrier of 15.0 kcal mol^{-1} (Figure 2). These two funnels correspond to structures containing the trans and cis isomers of the β-Ala-Pro peptide bond. The most stable isomers in each of the funnels are separated by less than 0.1 kcal mol^{-1}. All structures containing at least one of the other peptide groups in the cis conformation are at least 5.9 kcal mol^{-1} above the global minimum and separated from it by barriers of at least 18.3 kcal mol^{-1}. If these two funnels are in equilibrium at 298 K, one would expect 45% of the molecules to have all the peptide groups in trans conformations and 55% to have one cis peptide bond (Table 2).

For each arrangement of cis and trans peptide bonds, there are more than 50 minima. The funnel corresponding to a cis conformation in the β-Ala-Pro peptide bond splits into two subfunnels at 9.5 kcal mol^{-1} above the global minimum. The structures at the ends of these subfunnels (Figure 2b and 2c) differ by the orientation of the Pro-β-Ala peptide bond relative to the plane of the ring. The barrier to this rotation is relatively large because it requires concerted motion of many of the atoms in the macrocycle and the breaking of a transannular hydrogen bond. Smaller barriers separate minima that have different orientations of the other peptide groups relative to the ring or different arrangements of the β-alanine backbones. The

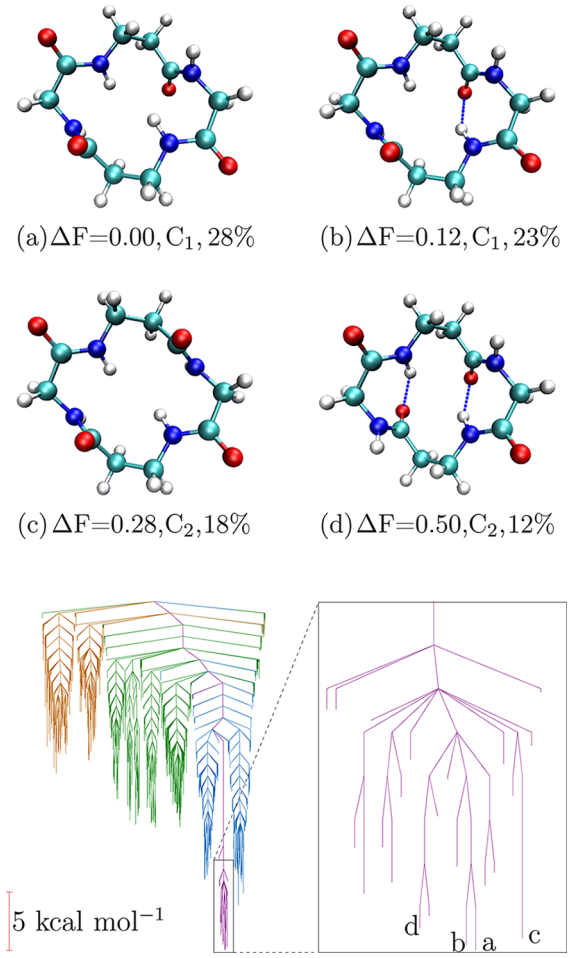

Figure 1. Four lowest-lying conformers of cyclo-[(β-Ala-Gly)$_2$] with their relative free energies, ΔF, in kcal mol^{-1}, point group symmetries, and the percentage occupancies summed over all symmetry-equivalent minima. Intramolecular hydrogen bonds are shown as dotted lines. Also shown is the free energy disconnectivity graph of cyclo-[(β-Ala-Gly)$_2$] in water at 298 K. The 616 minima and 2053 transition states accessible via transition states lower than 30 kcal mol^{-1} above the global minimum are shown. Insets are the 24 minima and 41 transition states accessible via transition states lower than 8 kcal mol^{-1} above the global minimum. Minima are colored by the number of trans peptide groups from orange (1) to purple (4).

smallest barriers of 1−2 kcal mol^{-1} correspond to pseudorotation[79,80] of the five-membered ring in the proline residue.

For the cis and trans isomers to be in equilibrium, the transition states linking them must be kinetically accessible. To the best of our knowledge, there are no experimental measurements of the rates of cis−trans isomerization for cyclic tetra-α/β-peptides. The closest compound for which experimental data are available is the cyclic pentapeptide cyclo-[Gly-Ala-Gly-Gly-Pro]. At 298 K, both conformers of the Gly-Pro peptide group are present in a 65:35 trans:cis ratio, with the lifetime of the cis isomer estimated to be between 2×10^{-2} and 3×10^{-1} s.[81] A free energy barrier of 14.3 kcal mol^{-1} (at 323 K) for cis−trans isomerization was obtained from saturation transfer NMR experiments.[82] Our calculations on the similar molecule cyclo-[Gly_4Pro], from the published database of stationary points,[12] show the cis and trans isomers in equilibrium but with the major isomer having a cis Gly-Pro peptide bond (Table 2). The calculated free-energy barrier for cis−trans isomerization in cyclo-[Gly_4-Pro] is 14.0 kcal mol^{-1},

dx.doi.org/10.1021/jp4043039 | J. Phys. Chem. B 2013, 117, 8122−8134

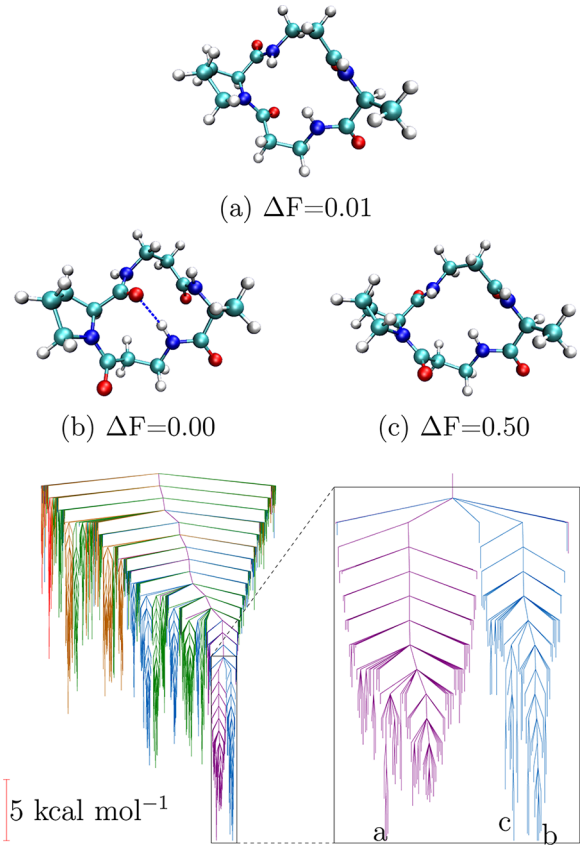

Figure 2. Low-lying structures of cyclo-[β-Ala-Ala-β-Ala-Pro] in water with their relative free energies, ΔF, in kcal mol^{-1}. Intramolecular hydrogen bonds are shown as dotted lines. Also shown is the free energy disconnectivity graph of cyclo-[β-Ala-Ala-β-Ala-Pro] in water at 298 K. The 1771 minima and 5293 transition states accessible via transition states lower than 30 kcal mol^{-1} above the global minimum are shown. Insets are the 190 minima and 428 transition states accessible via transition states lower than 15 kcal mol^{-1} above the global minimum. Minima are colored by the number of trans peptide groups from red (0) to purple (4).

Table 2. Calculated Populations of Conformations Grouped by the Number of Cis Peptide Groups in Some Cyclic Peptides in Water[a]

	number of cis peptides			
sequence	0	1	2	cis−trans barrier
cyclo-[Gly$_3$-Pro][12]	0.3%	98.2%	1.5%	13.6
cyclo-[Gly$_4$-Pro][12]	22.4%	77.6%	0.1%	14.0
cyclo-[β-Ala-Ala-β-Ala-Pro]	45.1%	54.9%	0.0%	15.0
cyclo-[β-Ala-Val-β-Ala-Pro]	42.3%	57.2%	0.5%	15.2

[a]Also shown are the energies of the lowest cis−trans transition states above the global minimum in kcal mol^{-1}.

which is close to the experimental barrier for cyclo-[Gly-Ala-Gly-Gly-Pro]. The barrier of 15.0 kcal mol^{-1} for cyclo-[β-Ala-Ala-β-Ala-Pro] leads to isomerization that is approximately 5 times slower at 298 K but is not sufficiently high to trap the cyclic peptide in either conformation.

To understand the effect of solvent polarity on the energy landscape of cyclo-[β-Ala-Ala-β-Ala-Pro], we have also performed discrete path sampling calculations in vacuo (Figure 3). In water, the most stable all-trans conformers have all of the peptide groups oriented perpendicular to the ring, with the C−O bond vectors pointing in the same direction (Figure 2a). In vacuo, the most stable all-trans conformers contain multiple intramolecular hydrogen bonds (Figure 3a). This rearrangement stabilizes the all-trans isomers in nonpolar conditions. The structures containing cis β-Ala-Pro peptide bonds are less able to respond to the change in solvent polarity because the oxygen atom in the cis peptide group is aligned equatorially and cannot be involved in an intramolecular hydrogen bond. The most stable structures in vacuo that contain cis peptide bonds (Figure 3b and 3c) only contain a single transannular hydrogen bond and are therefore less stable than the all-trans isomers. Decreasing the solvent polarity shifts the equilibrium population toward the all-trans arrangement of peptide groups. However, all of our experimental measurements were performed in polar solvents, and one would expect the conformational preferences to be closer to those calculated in water than those calculated in vacuo.

Energy Landscape of Cyclo-[β-Ala-Lys-β-Ala-Pro]. The number of possible conformations of the Lys side chain makes

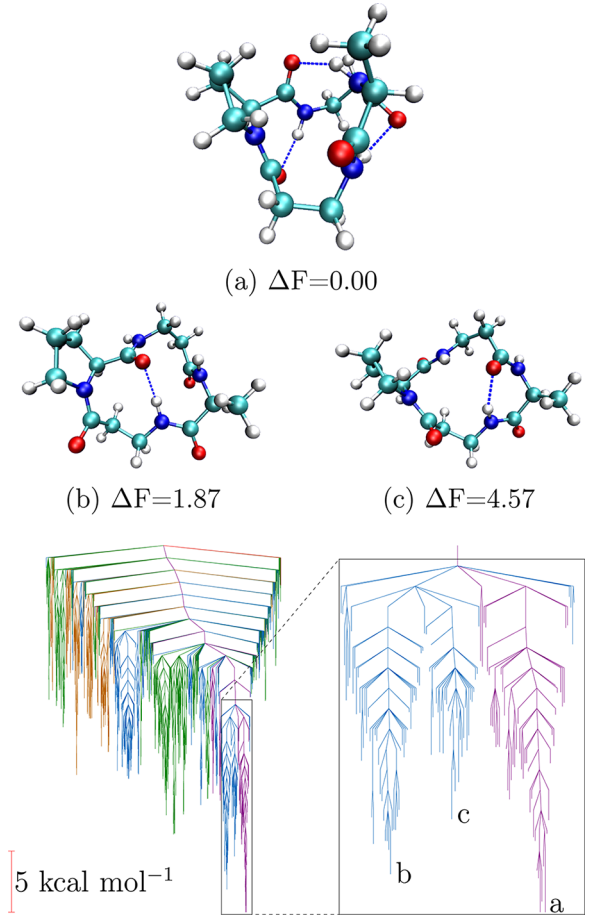

Figure 3. Low-lying structures of cyclo-[β-Ala-Ala-β-Ala-Pro] in vacuo with their relative free energies, ΔF, in kcal mol^{-1}. Intramolecular hydrogen bonds are shown as dotted lines. Also shown is the free energy disconnectivity graph of cyclo-[β-Ala-Ala-β-Ala-Pro] in vacuo at 298 K. The 1107 minima and 2429 transition states accessible via transition states lower than 30 kcal mol^{-1} above the global minimum are shown. Insets are the 138 minima and 284 transition states accessible via transition states lower than 18 kcal mol^{-1} above the global minimum. Minima are colored by the number of trans peptide groups from red (0) to purple (4).

dx.doi.org/10.1021/jp4043039 | J. Phys. Chem. B 2013, 117, 8122−8134

complete sampling of the cyclo-[β-Ala-Lys-β-Ala-Pro] energy landscape rather difficult. After 69 000 connection attempts, 8330 minima connected to the global minimum by transition states lower than 20 kcal mol^{-1} were located. If our estimate for the number of conformers of the Lys side chain is correct, one would expect about 40 000 minima. Despite this incomplete sampling, we present the results of these energy landscape calculations with the caveat that important low-lying minima could be missing. The energy landscape for cyclo-[β-Ala-Lys-β-Ala-Pro] is qualitatively similar to that seen for cyclo-[β-Ala-Ala-β-Ala-Pro]. The most stable structures containing trans (Figure 4a) and cis (Figure 4b) isomers of the β-Ala-Pro bond are similar in energy and separated by a free energy barrier of 15.2 kcal mol^{-1}. For the rest of this manuscript, we compare the experimental properties of cyclo-[β-Ala-Lys-β-Ala-Pro] to the energy landscape of cyclo-[β-Ala-Ala-β-Ala-Pro]. The incomplete energy landscape for cyclo-[β-Ala-Lys-β-Ala-Pro] is available as Supporting Information.

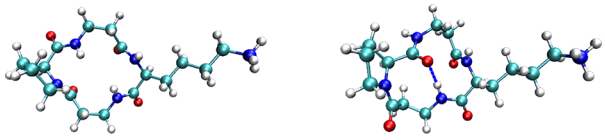

Figure 4. Lowest free energy structures of cyclo-[β-Ala-Lys-β-Ala-Pro] containing a trans (a) or cis (b) β-Ala-Pro peptide group with their relative free energies, ΔF, in kcal mol^{-1}. Intramolecular hydrogen bonds are shown as dotted lines.

NMR of Cyclo-[β-Ala-Lys-β-Ala-Pro]. The cyclic tetra-α/β-peptide cyclo-[β-Ala-Lys-β-Ala-Pro] was prepared by solid-phase peptide synthesis, anchored to the resin through the lysine side chain.[83,84] The cyclization of the peptide was performed on-resin.[85] The peptide was purified by reversed-phase C18-HPLC and characterized by MALDI-TOF, NMR, analytical C18-HPLC, and elemental analysis (NMR and HPLC data are available as Supporting Information). Both the analytical C18-HPLC and elemental analysis are consistent with a pure compound (>99%); however, the ^{1}H NMR spectra of a ca. 19 mM solution of cyclo-[β-Ala-Lys-β-Ala-Pro] in 90% H_2O/10% D_2O, MeOD-d_4, or DMSO-d_6 all display multiple sets of peaks. Despite these results, it did not prove possible to separate these species by HPLC. This is consistent with cyclo-[β-Ala-Lys-β-Ala-Pro] having multiple conformations that are in equilibrium but interconvert slowly on the NMR time scale.

Similarly, two sets of signals are observed in the ^{13}C NMR spectrum recorded in 90% H_2O/10% D_2O. The chemical shift difference between the Pro β-carbon and γ-carbon signal is sensitive to the conformation of the peptide bond.[86] The $\Delta\delta$ of 4.34 ppm for the major species indicates a trans β-Ala-Pro peptide bond, whereas the $\Delta\delta$ of 9.23 ppm for the minor species is consistent with a cis β-Ala-Pro peptide bond (Figure 5).[87]

NOESY NMR can be used to determine interproton distances and, hence, provide further information concerning the stereochemistry of the β-Ala-Pro bond. In the NOESY spectrum of cyclo-[β-Ala-Lys-β-Ala-Pro] in 90% H_2O/10% D_2O, no cross peaks were detected between protons H_α(β-Ala) (2.58 and 2.86 ppm) and H_α(Pro) (4.42 ppm) of species A, which would be expected for a stereoisomer with a cis β-Ala-Pro peptide bond. In contrast, cross peaks were detected

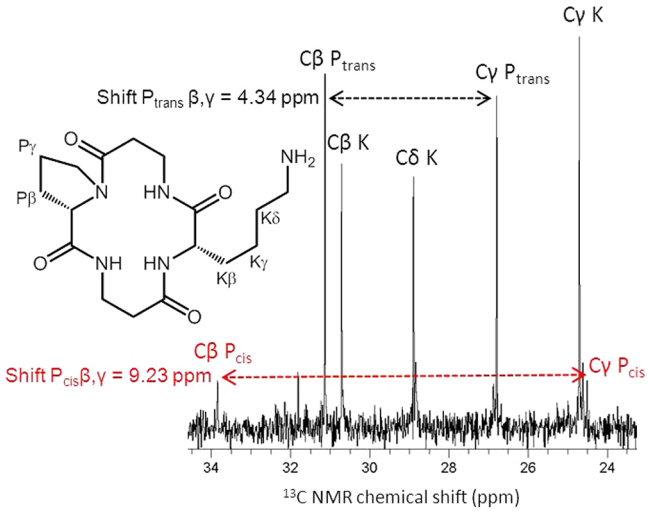

Figure 5. High-field region of the ^{13}C NMR spectrum of cyclo-[β-Ala-Lys-β-Ala-Pro] in 90% H_2O/10% D_2O. C_β-Pro and C_γ-Pro carbon signals for the two stereoisomers, species A (black) and species B (red), were assigned by HSQC NMR.

between protons H_α(β-Ala) and H_δ(Pro), consistent with a trans β-Ala-Pro peptide bond. However, the ^{1}H NMR spectrum is complicated by the fact that two H_δ(Pro) signals overlap with two of the four H_β(β-Ala) signals, for which geminal coupling with proton H_α(β-Ala) would also be expected. The resonance centered at 2.86 ppm, with an integration of one and assigned as H_α(β-Ala), gives rise to three cross couplings. Of these, two correspond to H_α(β-Ala)−H_β(β-Ala) coupling, and the third corresponds to H_α(β-Ala)−H_δ(Pro) coupling, consistent with the short distance between these two protons in the trans β-Ala-Pro conformation (Figure 6). We therefore conclude that, under these conditions (aqueous solution, 300 K), the major species A contains a trans β-Ala-Pro peptide bond. This is consistent with ^{1}H NMR assignments in the literature for isomers with differing Xaa-Pro peptide bond stereochemistry.[88−90]

^{1}H NMR spectra of cyclo-[β-Ala-Lys-β-Ala-Pro] recorded in H_2O:D_2O (90:10), MeOD-d_4, or DMSO-d_6 all reveal the presence of three distinct species, as determined by the number of resonances attributed to H_α(Lys), estimated by integration to be similar for the three different solvents used: 75:17:8 (90% H_2O/10% D_2O), 75:15:10 (MeOD-d_4), and 75:16:9 (DMSO-d_6). To account for the presence of a third species, one must consider that, in addition to the cis−trans stereoisomerism of the peptide bond, large barriers are also seen in reorientation of the peptide groups relative to the ring. When the β-Ala-Pro bond of cyclo-[β-Ala-Ala-β-Ala-Pro] is in the cis conformation, the two possible alignments of the next peptide group are separated by a large barrier (Figure 2b and 2c). It is possible that these isomers are responsible for the minor signals in the NMR. If the conformers responsible for these signals are at equilibrium, a 75:15:10 ratio corresponds to the conformers responsible for signals B and C having free energies 1.0 and 1.2 kcal mol^{-1} higher than conformer A, respectively. A distinction must be drawn between the free energies of individual minima, which we obtain from discrete path sampling, and the free energies of groups of minima, which we can obtain from NMR measurements. Variable-temperature ^{1}H NMR was performed for cyclo-[β-Ala-Lys-β-Ala-Pro] in MeOD-d_4 (233−303 K) and DMSO-d_6 (328−353 K). These experiments indicate that the

dx.doi.org/10.1021/jp4043039 | J. Phys. Chem. B 2013, 117, 8122−8134

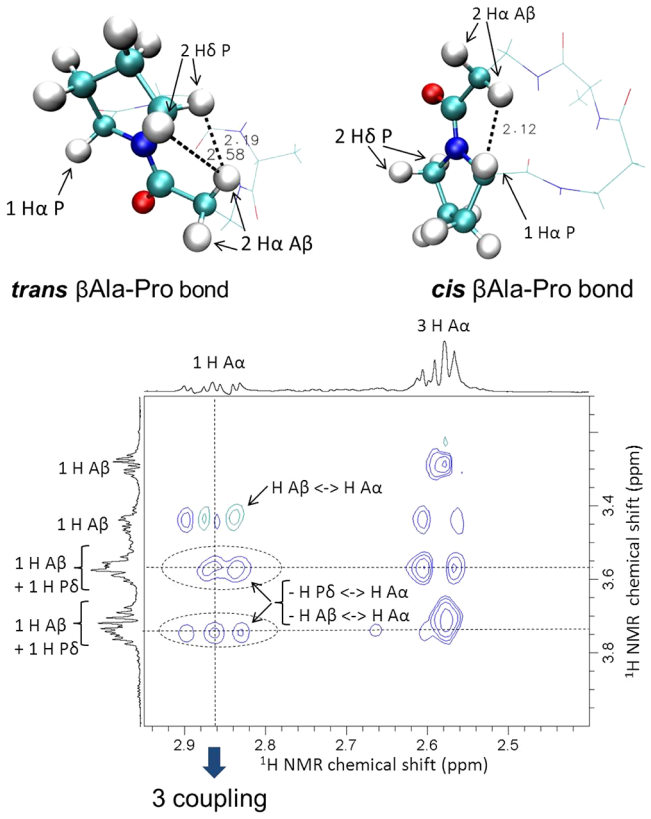

Figure 6. Backbone stereoisomer assignment for cyclo-[β-Ala-Lys-β-Ala-Pro] based on NOESY NMR. Shown are the structures of two stereoisomers with different configuration of the β-Ala-Pro peptide bond and the high-field region of the NOESY spectrum. Cross peaks can be attributed to either H_α(β-Ala)−H_δ(Pro) or H_α(β-Ala)−H_β(β-Ala). As one H_α(β-Ala) can only couple with two H_β(β-Ala), one of the two cross peaks circled can be attributed to H_α(β-Ala)−H_δ(Pro). Data recorded at 500 MHz; TPPI; 500 ms mixing time; 90% H_2O/10% D_2O; T = 300 K.

population of conformers in MeOD-d_4 and DMSO-d_6 remains largely unchanged over these temperature ranges (see Figure 7

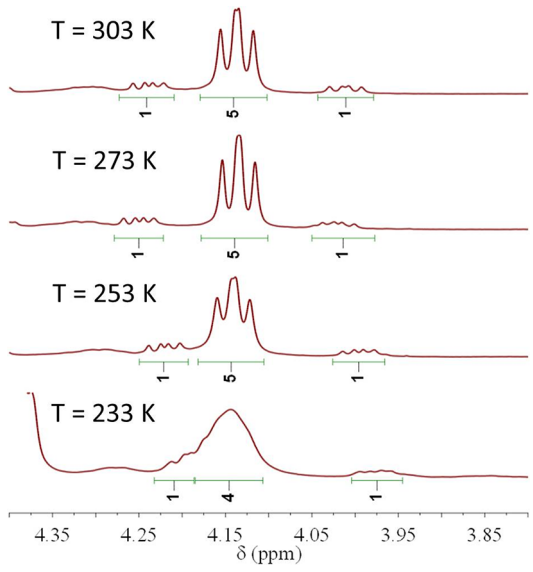

Figure 7. Variable-temperature ^{1}H NMR for cyclo-[β-Ala-Lys-β-Ala-Pro] in MeOD-d_4 showing the H_α(Lys) signal.

for MeOD-d_4 and Supporting Information for DMSO-d_6). Using the derived relative energies of the conformers responsible for signals A, B and C, one would expect ratios of 84:10:6 at 233 K and 70:18:12 at 353 K. The uncertainties in the integrated intensities of the minor signals are large enough that changes in the relative populations of this size are difficult to resolve. Comparing these NMR measurements to the calculated energy landscape of cyclo-[β-Ala-Ala-β-Ala-Pro], signal A corresponds to the funnel around the structure in Figure 2a. Signals B and C probably arise from the funnels centered on the structures in Figure 2b and Figure 2c, but we are unable to assign which structure corresponds to which signal. The NMR measurements give a slightly higher preference for the trans isomer than calculations. However, an error of less than 1 kcal mol^{-1} in the calculated energies would give the observed trans:cis ratio. This is in good agreement within the limitations of both NMR integration and force field calculations.

Circular Dichroism. Circular dichroism (CD) spectra of 0.8 mM cyclo-[β-Ala-Lys-β-Ala-Pro] were recorded at 298 K in various solvents (and solvent mixtures) with differing polarity and proticity. In water, the CD spectrum consists of a broad minimum centered at 217 nm, with a shoulder at 206 nm. As the polarity of the solvent decreases from H_2O to MeOH, and from MeOH to DCM, the shoulder at 206 nm disappears, and the minimum centered at 217 nm (θ = −8820 deg cm^2 dmol^{-1} res^{-1}, 100% H_2O) shifts to 226 nm and becomes more intense (θ = −13 640 deg cm^2 dmol^{-1} res^{-1}, 75% DCM/25% MeOH) (Figure 8). These results are consistent with the formation of a turn structure and the loss of hydrogen bonding to less protic solvents, similar to reports for related peptides.[36]

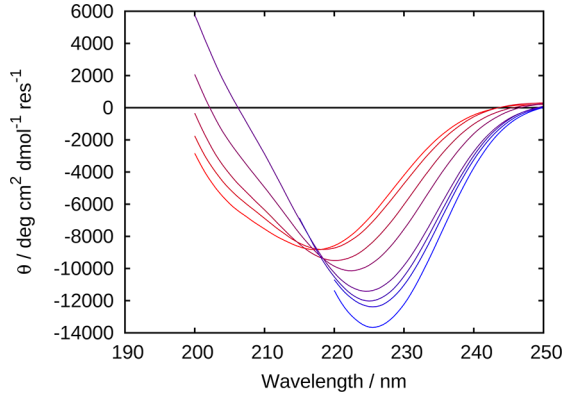

Figure 8. Influence of the solvent polarity on the CD spectrum of 0.8 mM cyclo-[β-Ala-Lys-β-Ala-Pro]. The lines correspond to H_2O (red), 75 H_2O:25 MeOH, 50 H_2O:50 MeOH, 25 H_2O:75 MeOH, MeOH, 75 MeOH:25 DCM, 50 MeOH:50 DCM, and 25 MeOH:75 DCM (blue). Ellipticity data are only displayed where the dynode voltage does not exceed 450 V.

The published CD spectrum for cyclo-[β-Ala-Ala-β-Ala-Pro] in water[36] is similar to our experimental CD spectrum for cyclo-[β-Ala-Lys-β-Ala-Pro], which suggests the backbones of both cyclic peptides adopt similar conformations. This provides some support for performing discrete path sampling on cyclo-[β-Ala-Ala-β-Ala-Pro] and subsequent use of the resulting backbone conformations to model peptides with more flexible side chains.

We have calculated the CD spectra of all the minima of cyclo-[β-Ala-Ala-β-Ala-Pro] using the matrix method. The CD

dx.doi.org/10.1021/jp4043039 | J. Phys. Chem. B 2013, 117, 8122−8134

spectrum corresponding to each of the low-lying funnels was calculated as a Boltzmann weighted sum of the minima in that funnel (Figure 9). The calculated CD spectrum of the all-trans isomer of cyclo-[β-Ala-Ala-β-Ala-Pro] is in good agreement with the experimental spectrum of cyclo-[β-Ala-Lys-β-Ala-Pro]. The CD spectra corresponding to most of the individual structures have a negative signal between 200 and 205 nm from the $\pi \rightarrow \pi^*$ transitions or at 222 nm from the $n \rightarrow \pi^*$ transition (see Supporting Information). The broad negative signal in the experimental spectrum is the sum of these two. The calculated CD spectra for minima with a cis β-Ala-Pro mainly have intense negative $\pi \rightarrow \pi^*$ signals and very little intensity in the $n \rightarrow \pi^*$ signal, which is in poorer agreement with the experimental spectrum.

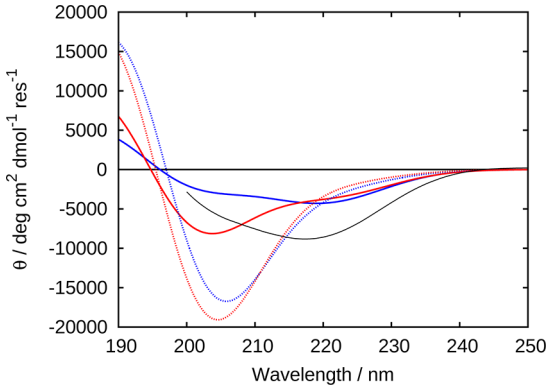

Figure 9. Boltzmann weighted averages of the calculated CD spectra of cyclo-[β-Ala-Ala-β-Ala-Pro] in water (red) and in vacuo (blue). The two lines for each solvent are for the trans β-Ala-Pro conformers (solid) and the cis β-Ala-Pro conformers (dotted). The experimental CD spectrum of cyclo-[β-Ala-Lys-β-Ala-Pro] in water is included for comparison (black).

The Boltzmann-weighted sum of the CD spectra calculated from the structures in the vacuum energy landscape shows a substantial decrease in the intensity of the $\pi \rightarrow \pi^*$ signal and a small increase in the intensity of the $n \rightarrow \pi^*$ signal. This change is in the same direction as observed for the experimental CD spectrum on decreasing the solvent polarity, although it does not show the full magnitude of the shift in the wavelength or the decrease in the ellipticity. The matrix method chromophore used in this calculation was parametrized in water and does not include the solvent-induced shift in the $n \rightarrow \pi^*$ transition. Therefore, the calculated change in the CD spectrum arises only due to the structural change.

We have also calculated CD spectra for all of the minima in the incomplete energy landscape of cyclo-[β-Ala-Lys-β-Ala-Pro]. The calculated CD spectra for the cis and trans funnels for cyclo-[β-Ala-Lys-β-Ala-Pro] are very similar to those seen for cyclo-[β-Ala-Ala-β-Ala-Pro] (Figure 10). This is an encouraging result, but it must be treated with caution because any low-lying minima that have not been sampled would affect the calculated spectra.

Energy Landscape of Cyclo-[β-Ala-Val-β-Ala-Pro]. Ala is a good model for Lys in our discrete path sampling calculations because the backbones of the Lys- and Ala-containing peptides are similar, but the Ala side chain has fewer degrees of freedom to explore. The isopropyl side chain of Val is also much less flexible than the side chain of Lys, which gives a much smaller number of stationary points to be explored.

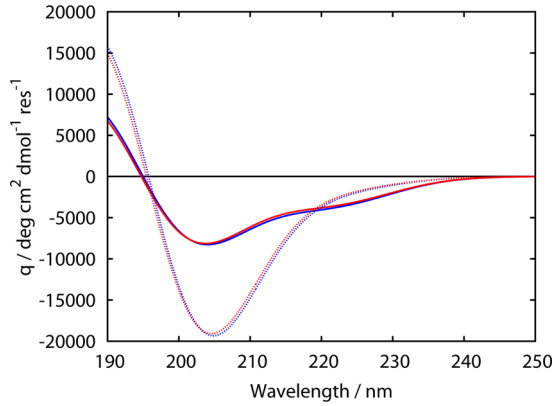

Figure 10. Boltzmann weighted averages of the calculated CD spectra cyclo-[β-Ala-Ala-β-Ala-Pro] (red) and cyclo-[β-Ala-Lys-β-Ala-Pro] (blue) in water. The two lines for each peptide are for the trans β-Ala-Pro conformers (solid) and the cis β-Ala-Pro conformers (dotted).

However, the Val side chain has steric bulk located close to the peptide backbone, which may lead to the conformations of the cyclic peptide ring being different from those of the Ala- or Lys-containing peptides.

Upon substituting Val for Ala, the additional rotational degree of freedom in the Val side chain leads to an increase in the number of stationary points compared to cyclo-[β-Ala-Ala-β-Ala-Pro], with the number of minima accessible by transition states lower than 20 kcal mol^{-1} increasing from 523 to 1422. The cyclo-[β-Ala-Val-β-Ala-Pro] energy landscape (Figure 11) has many similarities to that of cyclo-[β-Ala-Ala-β-Ala-Pro]. The conformers containing all-trans peptide groups and a single cis peptide in the β-Ala-Pro group are close in energy. The free energy barrier to isomerization of the β-Ala-Pro peptide bond is 15.2 kcal mol^{-1}, which is similar to cyclo-[β-Ala-Ala-β-Ala-Pro]. Some of the low-lying structures (Figure 11b and 11c) are also similar to those seen in cyclo-[β-Ala-Ala-β-Ala-Pro]. However, there are also some significant differences. In the most stable all-trans structure (Figure 11a), the Pro and Val side chains are both equatorial to the cyclic peptide ring. Structures similar to this in cyclo-[β-Ala-Ala-β-Ala-Pro] lie at least 2.8 kcal mol^{-1} above the global minimum. Additionally, the most stable isomer containing a second cis peptide (Figure 11d) is only 2.7 kcal mol^{-1} above the global minimum (compared to 5.9 kcal mol^{-1} in cyclo-[β-Ala-Ala-β-Ala-Pro]). The stability of both of these new structures may be due to the bulky isopropyl side chain preferring to adopt an equatorial position.

In the published crystal structure of cyclo-[β-Ala-Val-β-Ala-Pro],[39] the unit cell contains two molecules in slightly different conformations. Both of these have all of the peptide groups adopting the trans conformations and are arranged with all of the peptide groups aligned in roughly the same direction. The two structures differ by rotation of the Val side chain and a small change in the orientation of one of the peptide bonds. There is no intramolecular hydrogen bonding, but there is extensive intermolecular hydrogen bonding. Both of these are similar to that seen in Figure 11b, but with the orientation of the β-Ala-Val peptide flipped and no intramolecular hydrogen bond. The crystal structure is not the same as the most stable calculated aqueous-phase structures, but intermolecular hydrogen bonding and crystal packing interactions can have a substantial influence on the conformation of a molecule. Structures with alignments of the peptide groups similar to the

dx.doi.org/10.1021/jp4043039 | J. Phys. Chem. B 2013, 117, 8122−8134

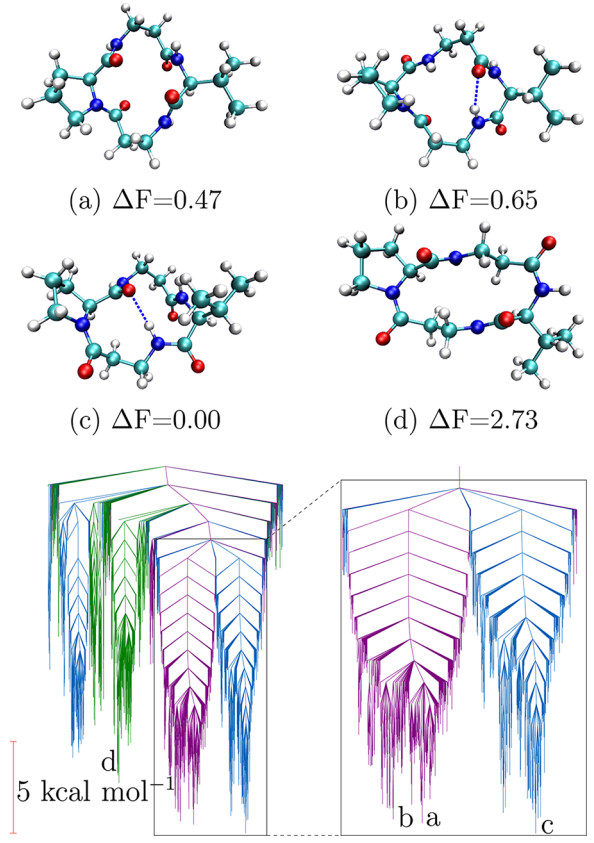

Figure 11. Low-lying structures of cyclo-[β-Ala-Val-β-Ala-Pro] in water with their relative free energies, ΔF, in kcal mol^{-1}. Intramolecular hydrogen bonds are shown as dotted lines. Also shown is the free energy disconnectivity graph of cyclo-[β-Ala-Val-β-Ala-Pro] in water at 298 K. The 1468 minima and 4145 transition states accessible via transition states lower than 20 kcal mol^{-1} above the global minimum are shown. Insets are the 673 minima and 2013 transition states accessible via transition states lower than 16 kcal mol^{-1} above the global minimum. Minima are colored by the number of trans peptide groups from green (2) to purple (4).

structures found by crystallography lie 1−2 kcal mol^{-1} above the global minimum.

CONCLUSIONS

The ring strain in cyclic tetra-α-peptides that is responsible for their unusual conformational behavior also makes them difficult to synthesize. Cyclic tetra-α/β-peptides are less strained and have cis/trans conformational preferences that are intermediate between the cyclic tetra-α-peptides and acyclic peptides.

NMR measurements on cyclo-[β-Ala-Lys-β-Ala-Pro] show the presence of a mixture of conformers that interconvert slowly on the NMR time scale. In the major isomer, all four peptide groups are in the trans conformation. Discrete path sampling calculations on the energy landscape of the simpler peptide, cyclo-[β-Ala-Ala-β-Ala-Pro], show the presence of two funnels corresponding to the trans and cis isomers of the β-Ala-Pro peptide bond. These funnels are very close in energy and are separated by a free energy barrier of 15 kcal mol^{-1}. The cis and trans isomers are likely to be in equilibrium at 298 K but interconverting slowly enough that they can be resolved by NMR spectroscopy. The similarity between the CD spectra of cyclo-[β-Ala-Lys-β-Ala-Pro] and cyclo-[β-Ala-Ala-β-Ala-Pro] is a good indication that the replacement of the Lys residue with Ala has little effect on the peptide backbone and justifies the use of Ala as a model for long flexible side chains.

The energy landscapes of cyclo-[β-Ala-Ala-β-Ala-Pro] and cyclo-[β-Ala-Val-β-Ala-Pro] exhibit some significant differences because the additional steric bulk of the Val side chain close to the peptide backbone has a substantial effect on the conformations of the ring. We have therefore demonstrated that though Ala is an appropriate substitute for amino acids with long flexible side chains it cannot be used to simplify the modeling of analogous peptides with amino acids where the side chains are sterically very demanding and in close proximity to the peptide backbone (such as Val).

The agreement between the experimental CD spectrum for cyclo-[β-Ala-Lys-β-Ala-Pro] in water and the calculated CD spectrum of the major isomer is good. However, our matrix method parameters are only fitted in water, and decreasing the polarity of the solvent leads to less good agreement. We intend to study the electronic spectroscopy of these cyclic peptides using TDDFT. To obtain good excitation energies for charge-transfer transitions, these calculations will be performed with long-range-corrected functionals.[91] It is also possible that hydrogen bonding to the solvent, which is not explicitly included in implicit solvent models, has some effect on the relative stabilities of the cyclic peptide conformations. We will undertake further calculations, either by adding a small number of explicit water molecules to the peptide or by performing molecular dynamics simulations starting from some of the low-lying minima, to understand the effect of intermolecular hydrogen bonding.

ASSOCIATED CONTENT

Supporting Information

Characterization data for cyclo-[β-Ala-Lys-β-Ala-Pro] including analytical HPLC and TOCSY, NOESY, HSCQ, and ^{1}H NMR spectra. Amber force field parameters for β-Ala. Calculated CD spectra for single minima on the cyclo-[β-Ala-Ala-β-Ala-Pro] free energy surface. Free energy disconnectivity graph for cyclo-[β-Ala-Lys-β-Ala-Pro]. This material is available free of charge via the Internet at http://pubs.acs.org.

AUTHOR INFORMATION

Corresponding Author

*E-mail: m.t.oakley@bham.ac.uk; a.f.a.peacock@bham.ac.uk; r.l.johnston@bham.ac.uk.

Notes

The authors declare no competing financial interest.

ACKNOWLEDGMENTS

MTO and RLJ thank Prof. Jonathan Hirst for providing the CD calculation software and acknowledge the Engineering and Physical Sciences Research Council, UK (EPSRC), for funding under Programme Grant EP/I001352/1. EO thanks the School of Chemistry at the University of Birmingham for a studentship. AFAP and EO thank The Royal Society for financial support. The computations described in this paper were performed using the University of Birmingham's BlueBEAR HPC service, which provides a High Performance Computing service to the University's research community. See http://www.birmingham.ac.uk/bear for more details. Some equipment used in this research was obtained through Birmingham Science City: Innovative Uses for Advanced Materials in the Modern World (West Midlands Centre for

Advanced Materials Project 2), with support from Advantage West Midlands (AWM) and partly funded by the European Regional Development Fund (ERDF).

REFERENCES

(1) Emmel, E. A.; Verweij, C. L.; Durand, D. B.; Higgins, K. M.; Lacy, E.; Crabtree, G. R. Cyclosporin A Specifically Inhibits Function of Nuclear Proteins Involved in T Cell Activation. *Science* **1989**, *246*, 1617−1620.

(2) Craik, D. J. Seamless Proteins Tie Up Their Loose Ends. *Science* **2006**, *311*, 1563−1564.

(3) Singh, S. B.; Zink, D. L.; Polishook, J. D.; Dombrowski, A. W.; Darkin-Rattray, S. J.; Schmatz, D. M.; Goetz, M. A. Apicidins: Novel Cyclic Tetrapeptides As Coccidiostats and Antimalarial Agents from Fusarium Pallidoroseum. *Tetrahedron Lett.* **1996**, *37*, 8077−8080.

(4) Kijima, M.; Yoshida, M.; Sugita, K.; Horinouchi, S.; Beppu, T. Trapoxin, an Antitumor Cyclic Tetrapeptide, Is an Irreversible Inhibitor of Mammalian Histone Deacetylase. *J. Biol. Chem.* **1993**, *268*, 22429−22435.

(5) Richman, M.; Wilk, S.; Chemerovski, M.; Wärmländer, S. K. T. S.; Wahlström, A.; Gräslund, A.; Rahimipour, S. In Vitro and Mechanistic Studies of an Antiamyloidogenic Self-Assembled Cyclic D,L-α-Peptide Architecture. *J. Am. Chem. Soc.* **2013**, *135*, 3474−3484.

(6) Pinet, E.; Neumann, J.-M.; Dahse, I.; Girault, G.; André, F. Multiple Interconverting Conformers of the Cyclic Tetrapeptide Tentoxin, [cyclo-(L-MeAla^1-L-Leu^2-MePhe[(Z)Δ]^3-Gly^4)], as Seen by Two-Dimensional ^{1}H-NMR spectroscopy. *Biopolymers* **1995**, *36*, 135−152.

(7) Kessler, H. Conformation and Biological Activity of Cyclic Peptides. *Angew. Chem., Int. Ed.* **1982**, *21*, 512−523.

(8) Loiseau, N.; Gomis, J.-M.; Santolini, J.; Delaforge, M.; André, F. Predicting the Conformational States of Cyclic Tetrapeptides. *Biopolymers* **2003**, *69*, 363−385.

(9) Che, Y.; Marshall, G. R. Engineering Cyclic Tetrapeptides Containing Chimeric Amino Acids as Preferred Reverse-Turn Scaffolds. *J. Med. Chem.* **2005**, *49*, 111−124.

(10) Rezai, T.; Bock, J. E.; Zhou, M. V.; Kalyanaraman, C.; Lokey, R. S.; Jacobson, M. P. Conformational Flexibility, Internal Hydrogen Bonding, and Passive Membrane Permeability: Successful in Silico Prediction of the Relative Permeabilities of Cyclic Peptides. *J. Am. Chem. Soc.* **2006**, *128*, 14073−14080.

(11) Bonnet, P.; Agrafiotis, D. K.; Zhu, F.; Martin, E. Conformational Analysis of Macrocycles: Finding What Common Search Methods Miss. *J. Chem. Inf. Model.* **2009**, *49*, 2242−2259.

(12) Oakley, M. T.; Johnston, R. L. Exploring the Energy Landscapes of Cyclic Tetrapeptides with Discrete Path Sampling. *J. Chem. Theory Comput.* **2013**, *9*, 650−657.

(13) Wales, D. J. Discrete Path Sampling. *Mol. Phys.* **2002**, *100*, 3285−3305.

(14) Wales, D. J. In *Energy Landscapes*; Wales, D. J., Ed.; Cambridge University Press: New York, 2003.

(15) Wales, D. J. Some Further Applications of Discrete Path Sampling to Cluster Isomerization. *Mol. Phys.* **2004**, *102*, 891−908.

(16) Poteau, R.; Trinquier, G. All-Cis Cyclic Peptides. *J. Am. Chem. Soc.* **2005**, *127*, 13875−13889.

(17) Jabs, A.; Weiss, M. S.; Hilgenfeld, R. Non-Proline Cis Peptide Bonds in Proteins. *J. Mol. Biol.* **1999**, *286*, 291−304.

(18) Zondlo, N. J. Aromatic−Proline Interactions: Electronically Tunable CH/π Interactions. *Acc. Chem. Res.* **2013**, *46*, 1039−1049.

(19) Wedemeyer, W. J.; Welker, E.; Scheraga, H. A. Proline Cis−Trans Isomerization and Protein Folding. *Biochemistry* **2002**, *41*, 14637−14644.

(20) Lummis, S. C. R.; Beene, D. L.; Lee, L. W.; Lester, H. A.; Broadhurst, R. W.; Dougherty, D. A. Cis−Trans Isomerization at a Proline Opens the Pore of a Neurotransmitter-Gated Ion Channel. *Nature* **2005**, *438*, 248−252.

(21) Sarkar, P.; Saleh, T.; Tzeng, S.-R.; Birge, R. B.; Kalodimos, C. G. Structural Basis for Regulation of The Crk Signaling Protein by a Proline Switch. *Nat. Chem. Biol* **2010**, *7*, 51−57.

(22) Cox, C.; Lectka, T. Solvent Effects on the Barrier to Rotation in Carbamates. *J. Org. Chem.* **1998**, *63*, 2426−2427.

(23) Brandts, J. F.; Halvorson, H. R.; Brennan, M. Consideration of the Possibility That the Slow Step in Protein Denaturation Reactions Is Due to Cis−Trans Isomerism of Proline Residues. *Biochemistry* **1975**, *14*, 4953−4963.

(24) Madison, V.; Schellman, J. Location of Proline Derivatives in Conformational Space. II. Theoretical Optical Activity. *Biopolymers* **1970**, *9*, 569−588.

(25) Fischer, G.; Wittmann-Liebold, B.; Lang, K.; Kiefhaber, T.; Schmid, F. X. Cyclophilin and Peptidyl-Prolyl Cis−Trans Isomerase Are Probably Identical Proteins. *Nature* **1989**, *337*, 476−478.

(26) Schmidt, U.; Langner, J. Cyclotetrapeptides and Cyclopentapeptides: Occurrence and Synthesis. *J. Pept. Res.* **1997**, *49*, 67−73.

(27) Zhang, L.; Tam, J. P. Metal Ion-Assisted Peptide Cyclization. *Tetrahedron Lett.* **1997**, *38*, 4375−4378.

(28) Haas, K.; Ponikwar, W.; Nöth, H.; Beck, W. Facile Synthesis of Cyclic Tetrapeptides from Nonactivated Peptide Esters on Metal Centers. *Angew. Chem., Int. Ed.* **1998**, *37*, 1086−1089.

(29) Horton, D. A.; Bourne, G. T.; Smythe, M. L. Exploring Privileged Structures: The Combinatorial Synthesis of Cyclic Peptides. *J. Comput.-Aided Mol. Des.* **2002**, *16*, 415−431.

(30) Davies, J. S. The Cyclization of Peptides and Depsipeptides. *J. Pept. Sci.* **2003**, *9*, 471−501.

(31) Bourne, G. T.; Coughlan, J.; Kaiser, S. M.; Jacobs, C. M.; Jones, A.; Ruhmann, A.; Turner, J. Y.; Smythe, M. L. Cyclic Tetrapeptides via the Ring Contraction Strategy: Chemical Techniques Useful for Their Identification. *Org. Biomol. Chem.* **2008**, *6*, 1386−1395.

(32) Fairweather, K. A.; Sayyadi, N.; Luck, I. J.; Clegg, J. K.; Jolliffe, K. A. Synthesis of All-L Cyclic Tetrapeptides Using Pseudoprolines as Removable Turn Inducers. *Org. Lett.* **2010**, *12*, 3136−3139.

(33) White, C. J.; Yudin, A. K. Contemporary Strategies for Peptide Macrocyclization. *Nature Chem.* **2011**, *3*, 509−524.

(34) Rutters, J. P. A.; Verdonk, Y.; de Vries, R.; Ingemann, S.; Hiemstra, H.; Levacher, V.; van Maarseveen, J. H. Synthesis of Strained Cyclic Peptides via an Aza-Michael-Acyl-Transfer Reaction Cascade. *Chem. Commun.* **2012**, *48*, 8084−8086.

(35) Brasuń, J.; Matera-Witkiewicz, A.; Ołdziej, S.; Pratesi, A.; Ginanneschi, M.; Messori, L. Impact of Ring Size on the Copper(II) Coordination Abilities of Cyclic Tetrapeptides. *J. Inorg. Biochem.* **2009**, *103*, 813−817.

(36) Vass, E.; Majer, Z.; Köhalmy, K.; Hollósi, M. Vibrational and Chiroptical Spectroscopic Characterization of γ-Turn Model Cyclic Tetrapeptides Containing Two β-Ala Residues. *Chirality* **2010**, *22*, 762−771.

(37) Pavone, V.; Lombardi, A.; D'auria, G.; Saviano, M.; Nastri, F.; Paolillo, L.; Di Blasio, B.; Redone, C. β-Alanine Containing Peptides: A Novel Molecular Tool for the Design of γ-Turns. *Biopolymers* **1992**, *32*, 173−183.

(38) Tamaki, M.; Akabori, S.; Muramatsu, I. Conformation of a Cyclic Tetrapeptide Containing Two Proline Residues. *Biopolymers* **1996**, *39*, 129−132.

(39) Di Blasio, B.; Lombardi, A.; D'Auria, G.; Saviano, M.; Isernia, C.; Maglio, O.; Paolillo, L.; Pedone, C.; Pavone, V. β-Alanine Containing Peptides: γ-Turns in Cyclotetrapeptides. *Biopolymers* **1993**, *33*, 621−631.

(40) Mazur, S.; Jayalekshmy, P. Chemistry of Polymer-Bound o-Benzyne. Frequency of Encounter between Substituents on Cross-Linked Polystyrenes. *J. Am. Chem. Soc.* **1979**, *101*, 677−683.

(41) Yan, B. Monitoring the Progress and the Yield of Solid-Phase Organic Reactions Directly on Resin Supports. *Acc. Chem. Res.* **1998**, *31*, 621−630.

(42) Berthelot, T.; Gonçalves, M.; Laïn, G.; Estieu-Gionnet, K.; Déléris, G. New Strategy Towards the Efficient Solid Phase Synthesis of Cyclopeptides. *Tetrahedron* **2006**, *62*, 1124−1130.

(43) Hirst, J. D.; Colella, K.; Gilbert, A. T. B. Electronic Circular Dichroism of Proteins from First-Principles Calculations. *J. Phys. Chem. B* **2003**, *107*, 11813−11819.
(44) Oakley, M. T.; Bulheller, B. M.; Hirst, J. D. First-Principles Calculations of Protein Circular Dichroism in the Far-Ultraviolet and Beyond. *Chirality* **2006**, *18*, 340−347.
(45) Bulheller, B. M.; Hirst, J. D. DichroCalc-Circular and Linear Dichroism Online. *Bioinformatics* **2009**, *25*, 539−540.
(46) Duan, Y.; Wu, C.; Chowdhury, S.; Lee, M. C.; Xiong, G.; Zhang, W.; Yang, R.; Cieplak, P.; Luo, R.; Lee, T.; Caldwell, J.; Wang, J.; Kollman, P. A Point-Charge Force Field for Molecular Mechanics Simulations of Proteins Based on Condensed-Phase Quantum Mechanical Calculations. *J. Comput. Chem.* **2003**, *24*, 1999−2012.
(47) Ponder, J. W.; Case, D. A. Force Fields for Protein Simulations. *Adv. Protein Chem.* **2003**, *66*, 27−85.
(48) Case, D. A.; Cheatham, T. E.; Darden, T.; Gohlke, H.; Luo, R.; Merz, K. M.; Onufriev, A. V.; Simmerling, C.; Wang, B.; Woods, R. J. The Amber Biomolecular Simulation Programs. *J. Comput. Chem.* **2005**, *26*, 1668−1688.
(49) Onufriev, A.; Bashford, D.; Case, D. A. Exploring Protein Native States and Large-Scale Conformational Changes with a Modified Generalized Born Model. *Proteins* **2004**, *55*, 383−394.
(50) Mulliken, R. S. Electronic Population Analysis on LCAO−MO Molecular Wave Functions. I. *J. Chem. Phys.* **1955**, *23*, 1833−1840.
(51) Valiev, M.; Bylaska, E. J.; Govind, N.; Kowalski, K.; Straatsma, T. P.; Van Dam, H. J. J.; Wang, D.; Nieplocha, J.; Apra, E.; Windus, T. L. NWChem: A Comprehensive and Scalable Open-Source Solution for Large Scale Molecular Simulations. *Comput. Phys. Commun.* **2010**, *181*, 1477−1489.
(52) Humphrey, W.; Dalke, A.; Schulten, K. VMD: Visual Molecular Dynamics. *J. Mol. Graphics* **1996**, *14*, 33−38.
(53) Wales, D. J. PATHSAMPLE: A program for refining and analysing kinetic transition networks. http://www-wales.ch.cam.ac.uk/PATHSAMPLE/.
(54) Wales, D. J.; Doye, J. P. K. Global Optimization by Basin-Hopping and the Lowest Energy Structures of Lennard-Jones Clusters Containing up to 110 Atoms. *J. Phys. Chem. A* **1997**, *101*, 5111−5116.
(55) Wales, D. J. GMIN: A Program for Finding Global Minima and Calculating Thermodynamic Properties from Basin-Sampling. http://www-wales.ch.cam.ac.uk/GMIN/.
(56) Trygubenko, S. A.; Wales, D. J. A Doubly Nudged Elastic Band Method for Finding Transition States. *J. Chem. Phys.* **2004**, *120*, 2082−2094.
(57) Wales, D. J. OPTIM: A program for characterising stationary points and reaction pathways. http://www-wales.ch.cam.ac.uk/OPTIM/.
(58) Munro, L. J.; Wales, D. J. Defect Migration in Crystalline Silicon. *Phys. Rev. B* **1999**, *59*, 3969−3980.
(59) Henkelman, G.; Jónsson, H. A Dimer Method for Finding Saddle Points on High Dimensional Potential Surfaces Using Only First Derivatives. *J. Chem. Phys.* **1999**, *111*, 7010−7022.
(60) Kumeda, Y.; Munro, L. J.; Wales, D. J. Transition States and Rearrangement Mechanisms from Hybrid Eigenvector-Following and Density Functional Theory. Application to C10H10 and Defect Migration in Crystalline Silicon. *Chem. Phys. Lett.* **2001**, *341*, 185−194.
(61) Carr, J. M.; Trygubenko, S. A.; Wales, D. J. Finding Pathways between Distant Local Minima. *J. Chem. Phys.* **2005**, *122*, 234903.
(62) Strodel, B.; Whittleston, C. S.; Wales, D. J. Thermodynamics and Kinetics of Aggregation for the GNNQQNY Peptide. *J. Am. Chem. Soc.* **2007**, *129*, 16005−16014.
(63) Becker, O. M.; Karplus, M. The Topology of Multidimensional Potential Energy Surfaces: Theory and Application to Peptide Structure and Kinetics. *J. Chem. Phys.* **1997**, *106*, 1495−1517.
(64) Wales, D. J.; Miller, M. A.; Walsh, T. R. Archetypal Energy Landscapes. *Nature* **1998**, *394*, 758−760.
(65) Krivov, S. V.; Karplus, M. Free Energy Disconnectivity Graphs: Application to Peptide Models. *J. Chem. Phys.* **2002**, *117*, 10894−10903.
(66) Evans, D. A.; Wales, D. J. Free Energy Landscapes of Model Peptides and Proteins. *J. Chem. Phys.* **2003**, *118*, 3891−3897.
(67) Amar, F. G.; Berry, R. S. The Onset of Nonrigid Dynamics and the Melting Transition in Ar_7. *J. Chem. Phys.* **1986**, *85*, 5943−5954.
(68) Wales, D. J. Coexistence in Small Inert Gas Clusters. *Mol. Phys.* **1993**, *78*, 151−171.
(69) Woody, R. W., Jr. Optical Rotation of Oriented Helices. III. Calculation of the Rotatory Dispersion and Circular Dichroism of the Alpha- and 3_{10}-Helix. *J. Chem. Phys.* **1967**, *46*, 4927−4945.
(70) Woody, R. W. Improved Calculation of the $n\pi^*$ Rotational Strength in Polypeptides. *J. Chem. Phys.* **1968**, *49*, 4797−4806.
(71) Bayley, P. M.; Nielsen, E. B.; Schellman, J. A. Rotatory Properties of Molecules Containing Two Peptide Groups: Theory. *J. Phys. Chem.* **1969**, *73*, 228−243.
(72) Besley, N. A.; Hirst, J. D. Theoretical Studies toward Quantitative Protein Circular Dichroism Calculations. *J. Am. Chem. Soc.* **1999**, *121*, 9636−9644.
(73) Oakley, M. T.; Hirst, J. D. Charge-Transfer Transitions in Protein Circular Dichroism Calculations. *J. Am. Chem. Soc.* **2006**, *128*, 12414−12415.
(74) Nielsen, E. B.; Schellman, J. A. The Absorption Spectra of Simple Amides and Peptides. *J. Phys. Chem.* **1967**, *71*, 2297−2304.
(75) Oakley, M. T.; Guichard, G.; Hirst, J. D. Calculations on the Electronic Excited States of Ureas and Oligoureas. *J. Phys. Chem. B* **2007**, *111*, 3274−3279.
(76) Tozer, D. J.; Amos, R. D.; Handy, N. C.; Roos, B. O.; Serrano-Andrés, L. Does Density Functional Theory Contribute to the Understanding of Excited States of Unsaturated Organic Compounds? *Mol. Phys.* **1999**, *97*, 859−868.
(77) Kappel, J. C.; Barany, G. Methionine Anchoring Applied to the Solid-Phase Synthesis of Lysine-Containing 'Head-to-Tail' Cyclic Peptides. *Lett. Pept. Sci.* **2003**, 119−125.
(78) Chan, W. C.; White, P. D. *Fmoc solid phase peptide synthesis: a practical approach*; Oxford University Press: New York, 2000.
(79) Altona, C.; Sundaralingam, M. Conformational Analysis of the Sugar Ring in Nucleosides and Nucleotides. New Description Using the Concept of Pseudorotation. *J. Am. Chem. Soc.* **1972**, *94*, 8205−8212.
(80) Westhof, E.; Sundaralingam, M. A Method for the Analysis of Puckering Disorder in Five-Membered Rings: The Relative Mobilities of Furanose and Proline Rings and Their Effects on Polynucleotide and Polypeptide Backbone Flexibility. *J. Am. Chem. Soc.* **1983**, *105*, 970−976.
(81) Meraldi, J. P.; Schwyzer, R.; Tun-Kyi, A.; Wüthrich, K. Conformational Studies of Cyclic Pentapeptides by Proton Magnetic Resonance Spectroscopy. *Helv. Chim. Acta* **1972**, *55*, 1962−1973.
(82) Grathwohl, C.; Wüthrich, K. NMR Studies of the Rates of Proline Cis−Trans Isomerization in Oligopeptides. *Biopolymers* **1981**, *20*, 2623−2633.
(83) Sabatino, G.; Chelli, M.; Mazzucco, S.; Ginanneschi, M.; Papini, A. M. Cyclisation of Histidine Containing Peptides in the Solid-Phase by Anchoring the Imidazole Ring to Trityl Resins. *Tetrahedron Lett.* **1999**, *40*, 809−812.
(84) Alcaro, M. C.; Sabatino, G.; Uziel, J.; Chelli, M.; Ginanneschi, M.; Rovero, P.; Papini, A. M. On-Resin Head-to-Tail Cyclization of Cyclotetrapeptides: Optimization of Crucial Parameters. *J. Pept. Sci.* **2004**, *10*, 218−228.
(85) Fridkin, M.; Patchornik, A.; Katchalski, E. A Synthesis of Cyclic Peptides Utilizing High Molecular Weight Carriers. *J. Am. Chem. Soc.* **1965**, *87*, 4646−4648.
(86) Jardetzky, O.; Roberts, G. C. K. *NMR in molecular biology*; Academic Press: New York, 1981.
(87) Dorman, D. E.; Bovey, F. A. Carbon-13 Magnetic Resonance Spectroscopy. Spectrum of Proline in Oligopeptides. *J. Org. Chem.* **1973**, *38*, 2379−2383.
(88) Deber, C. M.; Bovey, F. A.; Carver, J. P.; Blout, E. R. Nuclear Magnetic Resonance Evidence for Cis-Peptide Bonds in Proline Oligomers. *J. Am. Chem. Soc.* **1970**, *92*, 6191−6198.

(89) Deber, C. M.; Fossel, E. T.; Blout, E. R. Cyclic Peptides. VIII. Carbon-13 and Proton Nuclear Magnetic Resonance Evidence for Slow 'Cis−Trans' Rotation in a Cyclic Tetrapeptide. *J. Am. Chem. Soc.* **1974**, *96*, 4015−4017.
(90) Francart, C.; Wieruszeski, J. M.; Tartar, A.; Lippens, G. Structural and Dynamic Characterization of Pro Cis/Trans Isomerization in a Small Cyclic Peptide. *J. Am. Chem. Soc.* **1996**, *118*, 7019−7027.
(91) Yanai, T.; Tew, D. P.; Handy, N. C. A New Hybrid Exchange-Correlation Functional Using the Coulomb-Attenuating Method (CAM-B3LYP). *Chem. Phys. Lett.* **2004**, *393*, 51−57.